

# Instabilities in Explicit Super-Time-Stepping Schemes

Fabien Le Floc'h

International Conference on Computational Finance  
CWI, April 2024

# Why STS Schemes?

- stability criteria much more practical than explicit Euler for diffusion equations:

$$s \propto \frac{1}{\sqrt{\Delta t_{\text{explicit}}}}$$

where  $\Delta t_{\text{explicit}} \propto \frac{m^2}{n}$  with  $m$  number of space-steps,  $n$  number of time-steps,  $s$  number of stages.

- still explicit: easy to adapt to multi-dimensional problems and non-linear problems

Diffusion equation:

$$\frac{\partial f}{\partial t}(x, t) = \mathcal{L}(f(x, t), x, t) . \quad (1)$$

And the RKC, RKL, RKG schemes read (Verwer 1996, Meyer 2014)

$$\hat{f}^0 = f(t_j) , \quad (2a)$$

$$\hat{f}^1 = \hat{f}^0 + \tilde{\lambda}_1 k_j \mathcal{L}(\hat{f}^0) , \quad (2b)$$

$$\begin{aligned} \hat{f}^\eta = & \lambda_\eta \hat{f}^{\eta-1} + \nu_\eta \hat{f}^{\eta-2} + (1 - \lambda_\eta - \nu_\eta) \hat{f}^0 \\ & + \tilde{\lambda}_\eta k_j \mathcal{L}(\hat{f}^{\eta-1}) + \tilde{\gamma}_\eta k_j \mathcal{L}(\hat{f}^0) , \quad \text{for } 2 \leq \eta \leq s , \end{aligned} \quad (2c)$$

$$f(t_{j-1}) = \hat{f}^s , \quad (2d)$$

# Some STS schemes

## Runge-Kutta-Chebyshev

Let

$$b_\eta = \frac{P_\eta''(w_0)}{P_\eta'(w_0)^2}, \quad a_\eta = 1 - b_\eta P_\eta(w_0).$$

For RKC, we have for  $2 \leq \eta \leq s$

$$\begin{aligned} \lambda_\eta &= 2 \frac{b_\eta}{b_{\eta-1}} w_0, & \tilde{\lambda}_\eta &= \frac{\lambda_\eta}{w_0} w_1, \\ \nu_\eta &= -\frac{b_\eta}{b_{\eta-2}}, & \tilde{\gamma}_\eta &= -a_{\eta-1} \tilde{\lambda}_\eta, \end{aligned}$$

and  $w_0 = 1 + \epsilon/s^2$ ,  $b_0 = b_1 = 1/3$ ,  $a_0 = 1 - b_0 w_0$ ,  $\tilde{\lambda}_1 = b_1 w_1$ ,  
 $w_1 = P_s'(w_0)/P_s''(w_0)$ .

# Some STS schemes

## Runge-Kutta-Legendre

$a_\eta$  and  $b_\eta$  are explicit for RKL (no damping)

$$b_\eta = \frac{\eta^2 + \eta - 2}{2\eta(\eta + 1)}, \quad a_\eta = 1 - b_\eta,$$

For RKL, we have for  $2 \leq \eta \leq s$

$$\lambda_\eta = \frac{2\eta - 1}{\eta} \frac{b_\eta}{b_{\eta-1}} w_0, \quad \nu_\eta = -\frac{\eta - 1}{\eta} \frac{b_\eta}{b_{\eta-2}},$$

and  $w_0 = 1$ ,  $b_0 = b_1 = 1/3$ ,  $a_0 = 1 - b_0 w_0$ ,  $\tilde{\lambda}_1 = b_1 w_1$ ,  
 $w_1 = \frac{4}{s^2 + s - 2}$ .

# Some STS schemes

## Runge-Kutta-Gegenbauer

For RKG  $a_\eta$  and  $b_\eta$  are explicit and read

$$b_\eta = \frac{4(\eta - 1)(\eta + 4)}{3\eta(\eta + 1)(\eta + 2)(\eta + 3)}, \quad a_\eta = 1 - \frac{(\eta + 1)(\eta + 2)}{2} b_\eta,$$

For RKG, we have for  $2 \leq \eta \leq s$

$$\lambda_\eta = \frac{2\eta + 1}{\eta} \frac{b_\eta}{b_{\eta-1}} w_0, \quad \nu_\eta = -\frac{\eta + 1}{\eta} \frac{b_\eta}{b_{\eta-2}},$$

and  $w_0 = 1$ ,  $b_0 = 1$ ,  $b_1 = 1/3$ ,  $a_0 = 1 - b_0 w_0$ ,  $\tilde{\lambda}_1 = w_1$ ,  
 $w_1 = \frac{6}{(s+4)(s-1)}$ .

Damping  $\epsilon = 2/13$  suggested in Verwer (1996). CMP = monotone with space varying coefficient.

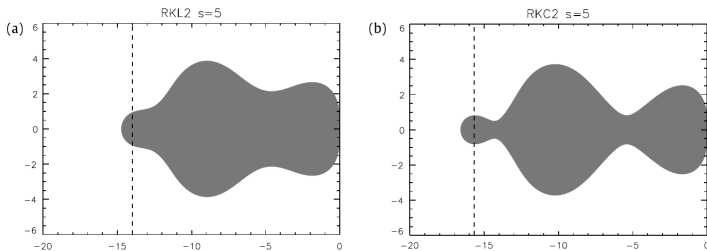


**Fig. 11.** (a) Shows the domain of stability in the complex plane for the  $s = 5$  RKL2 scheme. (b) Shows the same for the damped  $s = 5$  RKC2 scheme. The dotted line represents the maximum stable time step according to the respective method.

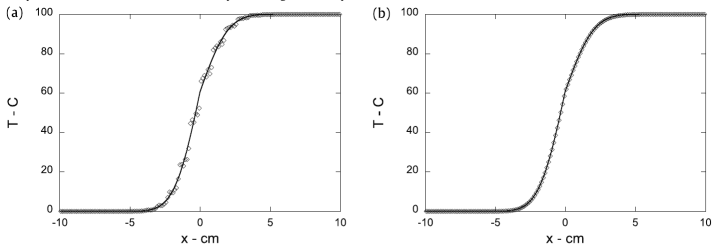
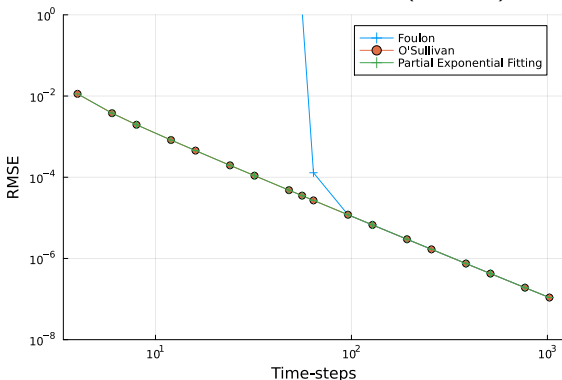


**Fig. 1.** (a) Shows the aluminum/copper heat conduction solution for the damped 7-stage RKC2 scheme, with damping coefficient  $\epsilon = 2/13$ . (b) Shows the solution for the 7-stage RKL2 scheme.

# Instabilities on the Heston PDE

$$\frac{\partial f}{\partial t} = \frac{vx^2}{2} \frac{\partial^2 f}{\partial x^2} + \rho\sigma xv \frac{\partial^2 f}{\partial x \partial v} + \frac{\sigma^2 v}{2} \frac{\partial^2 f}{\partial v^2} + (r-q)x \frac{\partial f}{\partial x} + \kappa(\theta-v) \frac{\partial f}{\partial v} - rf,$$

for  $0 \leq t \leq T$ ,  $x > 0$ ,  $v > 0$ , with  $f(T, x, v) = F(x)$ .



Convergence in time of the RKC scheme with  $\epsilon = 10$ , with the different choices of upwinding with  $m = 100$ ,  $n = 50$ .



# Instabilities on the Heston PDE

## Upwinding

Different zones:

- Foulon and In't Hout (2010): three points upwinding is used at  $v = 0$  and for  $v > 1$ .
- Le Floc'h (2019): exponential fitting is used when the Peclet number  $P > 2$  and single-sided differences are used at the boundaries  $x_{\min}, x_{\max}, v_{\min}, v_{\max}$ .
- O'Sullivan and O'Sullivan (2013) follow Ikonen and Toivanen (2007): one-sided upwinding applied anywhere the PDE becomes convection dominated.

*We use central finite differences as much as possible, but when they lead to a positive codiagonal element we employ first-order accurate one-sided differences for the convection terms, that is, for the spatial first-order partial derivative terms*

# Instabilities on the Heston PDE

## Exponential Fitting

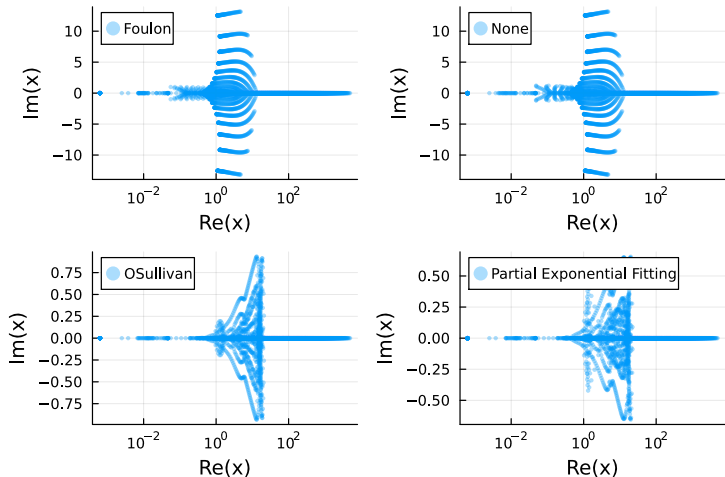
The cell Péclet number  $P =$  ratio of the advection coefficient towards the diffusion coefficient in a cell .When  $P > 2$  , the solution may explode.

$$P_{i,j}^x(\beta_{i,j}^x) = \frac{2h_i}{\beta_{i,j}^x v_j x_i} (r_i - q_i), \quad P_{i,j}^v(\beta_{i,j}^v) = \frac{2w_j \kappa (\theta - v_j)}{\beta_{i,j}^v \sigma^2 v_j}.$$

$$\beta_{i,j}^x = \frac{P_{i,j}^x(1)}{2 \tanh\left(\frac{P_{i,j}^x(1)}{2}\right)}, \quad \beta_{i,j}^v = \frac{P_{i,j}^v(1)}{2 \tanh\left(\frac{P_{i,j}^v(1)}{2}\right)},$$

# Instabilities on the Heston PDE

## Eigenvalues



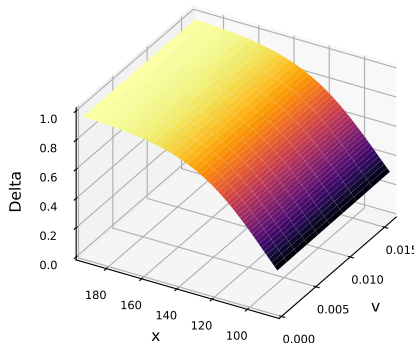
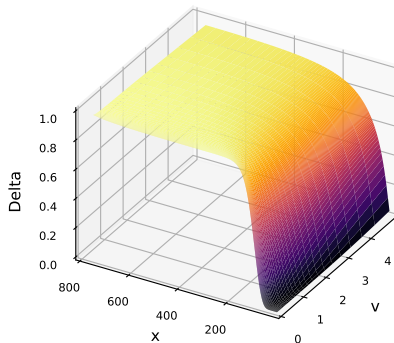
Eigenvalues of the discretization matrix with  $l = 16$ ,  $m = 100$ ,  $n = 50$  using different upwinding choices. Note the imaginary axis range difference

# Instabilities on the Heston PDE

## Oscillations - RKC

Delta by forward difference for  $l = 10$  time-steps and partial exponential fitting on the grid  $m = 100, n = 50$

RKC with damping shift  $\epsilon = 10$ . No oscillations are visible near  $v = 0$ .

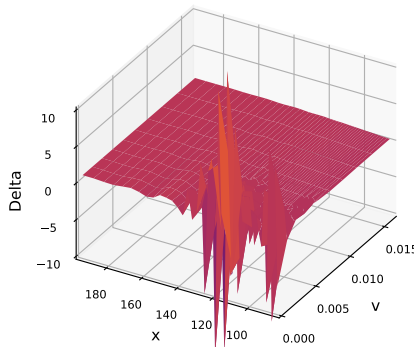
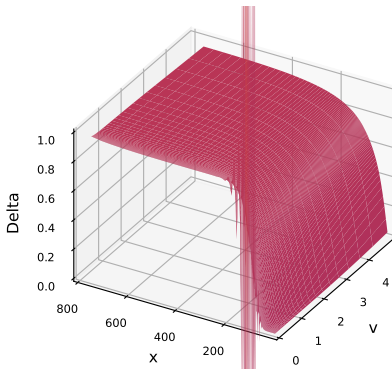


(Left: full grid, Right: zoom on small  $v$ )

# Instabilities on the Heston PDE

## Oscillations - RKL

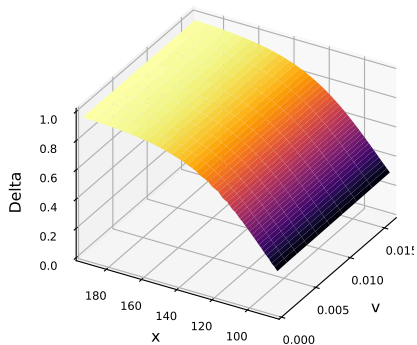
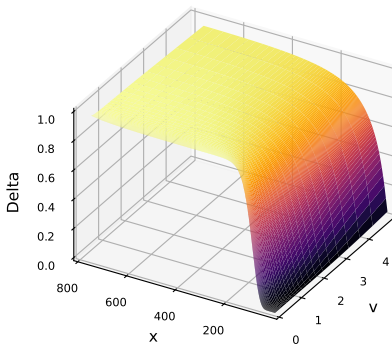
RKL presents oscillations for a small number of steps. Not RKC with large damping



# Instabilities on the Heston PDE

## Oscillations - RKG

RKG: Very small oscillations are visible at  $v = 0$ .

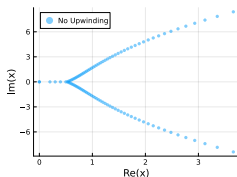
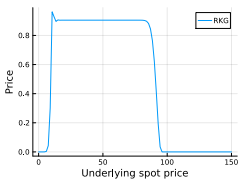
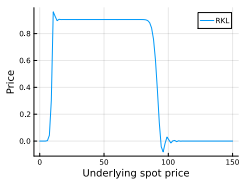


# Instabilities on the Black-Scholes PDE

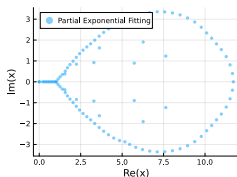
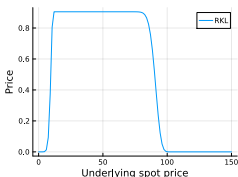
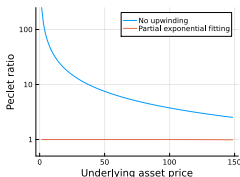
## Oscillations

Small volatility  $\sigma = 2\%$  and large interest rate  $r = 10\%$ .  
Expiry barrier option which pays \$1 if  $X(T)$  is between 10 and 100 and zero otherwise,  $T = 1$ .  $l = 100$  time-steps on a uniform grid with  $m = 100$  space steps.

No upwinding (RKL, RKG or TR-BDF2, Eigenvalues)



Exponential fitting ( $P$ , RKL, Eigenvalues)

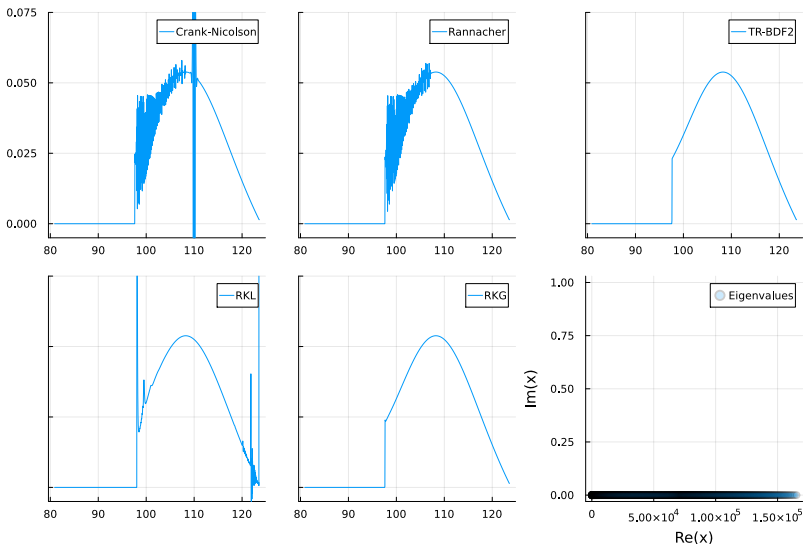


upwinding important, solves the two oscillations.

# Instabilities on the Black-Scholes PDE

## Gamma of American Put - The need for damping

100 time-steps and 1000 space steps with  $x_{\min} = 80.89$  and  $S_{\max} = 123.59$  (3 standard deviations with  $\sigma = 10\%$ ,  $r = 1\%$ ). American option with strike  $K = 110$ ,  $T = 0.5$ . Peclet  $P < 10^{-3}$





# Ghost points

1210 Part Six numerical methods and programs

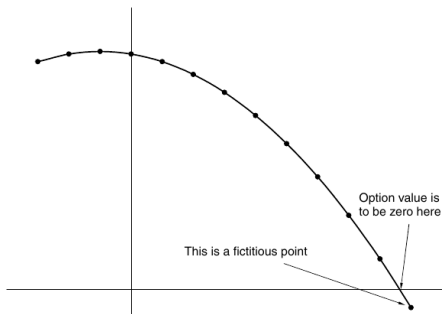


**Figure 77.6** A fictitious point, introduced to ensure accuracy in a barrier option boundary condition.

This condition can be approximated by ensuring that the straight line connecting the option values at the two grid points straddling the barrier has the value  $f$  at the barrier. Then a good discrete version of this boundary condition is

$$V_i^k = \frac{1}{\alpha} (f - (1 - \alpha)V_{i-1}^k)$$

where

$$\alpha = \frac{S_u - (I - 1)\delta S}{\delta S}.$$

This is accurate to  $O(\delta S^2)$ , the same order of accuracy as in the approximation of the  $\mathcal{C}$

# Ghost points with explicit schemes?

## Stability condition

Black-Scholes PDE, uniform discretization. When  $r = q = 0$ ,

$$\delta t \leq \frac{4\delta S^2}{\sigma_k^2 S_{u-1}^2 \left( 3 + \frac{S_u - L^+}{L^+ - S_{u-1}} \right)}.$$

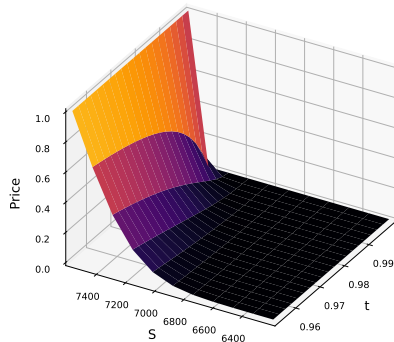
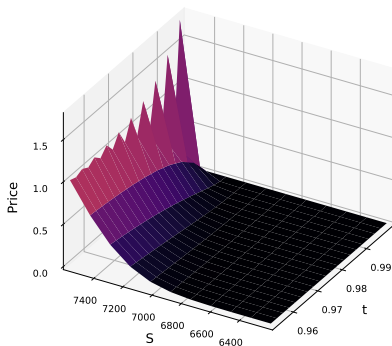
Increasingly stringent as the grid point  $S_{u-1}$  moves towards  $L^+$ .  
Let  $\epsilon = L^+ - S_{u-1}$ , we have

$$\frac{4\delta S^2}{\sigma_k^2 S_{u-1}^2 \left( 3 + \frac{\delta S - \epsilon}{\epsilon} \right)} = \frac{4\delta S}{\sigma_k^2 S_{u-1}^2} \epsilon + \mathcal{O}(\epsilon^2).$$

# What about implicit schemes?

Price of a one-touch option obtained by the Crank-Nicolson scheme on the finite difference grid, for  $M = 100$  space-steps and  $N = 400$  time-steps, close to the expiry and the barrier level.

Uniform with ghost point vs. Stretched, barrier on grid



TR-BDF2 no oscillations at all (excluding first two time-steps).

# Instabilities of STS schemes

## Conclusions

- STS are interesting in many practical cases
- upwinding important but lack of damping may be a concern.
- Ghost point technique should not be used with STS.
- RKL, RKG interesting properties, but would those also be achievable with a proper choice of damping coefficient in RKC?
- Don't use too many stages?

- Ikonen and Toivanen (2007) Efficient Numerical Methods for Pricing American Options Under Stochastic Volatility
- In't Hout and Foulon (2010) ADI Finite difference schemes for option pricing in the Heston model with correlation
- Le Floc'h (2019) Pricing American options with the Runge-Kutta-Legendre finite difference scheme
- Le Floc'h (2023) Instabilities of Super-Time-Stepping Methods on the Heston Stochastic Volatility Model
- Le Floc'h (2023) Instabilities of explicit finite difference schemes with ghost points on the diffusion equation
- Meyer, Balsara, Aslam (2014) A stabilized Runge–Kutta–Legendre method for explicit super-time-stepping of parabolic and mixed equations
- Verwer (1996) Explicit Runge-Kutta methods for parabolic partial differential equations
- Wilmott (2000) Paul Wilmott on Quantitative Finance